

Evaluation of the effect of Ag- doping ZnO microstructure on optical and structural properties and application in photocatalytic properties

Nedal A. Hussain¹, Osama AbdulAzeez Dakhil¹, Luma Y. Abbas^{1*}

¹Department of Physics, College of Science Mustansiriyah University, 10052 Baghdad, Iraq.

*Correspondent contact: ilmaphysics2203@uomustansiriyah.edu.iq

Article Info

Received
28/01/2023

Revised
28/02/2023

Accepted
08/03/2023

Published
30/09/2023

ABSTRACT

The chemical bath deposition technique was successful in producing silver-doped ZnO thin films. On the glass substrates, pure and silver-doped ZnO thin films have been deposited. By using a variety of sophisticated techniques, including X-ray Diffraction (XRD), Field emission Scanning Electron Microscope (FESEM), UV-vis spectrophotometer, and photoluminescence (PL) spectroscopy, the generated pure and Ag-doped ZnO thin films were studied. According to X-ray analysis, Ag-doped ZnO crystallized as a hexagonal wurtzite structure with a preference for growth in the (002) planes, the pure and Ag-doped ZnO's hexagonal wurtzite structures provided evidence for the microparticles' luminescent characteristics. The analysis of the methylene blue degradation revealed that the best photocatalytic response was displayed by the doped ZnO thin film. All thin films' optical bandgaps were broad, and they generally decrease after more doping, it was possible to determine that the particles were elliptical and rod-shaped and that their diameters were on the order of micrometers. for both the doped and pure ZnO microparticles were seen to exist. The outcome shows that the produced microparticles' average grain diameter was determined to be (15,20.5,14.5) μm , with noteworthy band gaps of 3.39,3.34 eV, and 3.08 eV, respectively.

KEYWORDS: ZnO, microparticles, silver doping, absorbance, photoluminescence, photocatalytic.

الخلاصة

تم تحضير أغشية ZnO الرقيقة قبل وبعد التشويب بالفضة بطريقة الترسيب بالحمام الكيميائي. تم ترسيب أغشية ZnO الرقيقة النقية والمشوبة بالفضة على قواعد زجاجية. وباستخدام مجموعة من التقنيات بما في ذلك حيود الأشعة السينية (XRD)، ومجهر المسح الإلكتروني (FESEM)، ومقياس الطيف الضوئي بالأشعة المرئية وفوق البنفسجية، والتحليل الطيفي الضوئي (PL)، تمت دراسة أغشية ZnO الرقيقة النقية والمشوبة بالفضة. وفقاً لتحليل الأشعة السينية نلاحظ تبلور أكسيد الزنك المشوب Ag-doped باعتباره هيكل wurtzite سداسي الأضلاع مع أفضل نمو في الاتجاهات (002). في درجة حرارة الغرفة، قدمت هياكل Wurtzite السداسية النقية والمشوبة دليلاً على خصائص الطيف الضوئي للجسيمات الدقيقة. أظهر تحليل تحلل الميثيلين الأزرق أن أفضل استجابة تحفيز ضوئي كانت للغشاء الرقيق ZnO بعد التشويب بالفضة. كانت جميع فجوات الطاقة للأغشية الرقيقة واسعة، وتقلصت عموماً بعد زيادة نسبة التشويب بالفضة، بمساعدة الصور المجهرية، تم تحديد أن الجسيمات كانت بيضاوية وكروية واعمد الشكل وأن أقطارها كانت في حدود بضعة ميكرون. أظهرت النتائج أن متوسط قطر الحبيبات للجسيمات الدقيقة المنتجة كان بحدود (15, 20.5, 14.5) ميكرون، مع فجوات نطاق ملحوظة تبلغ 3.3, 3.18 فولت، و 3.08 فولت على التوالي.

INTRODUCTION

Zinc Oxide (ZnO) exhibits a wide band gap of 3.37 eV and a significant exciton binding energy of 60 meV at ambient temperature [1]. Because of good electrical optical, piezoelectric, non-

toxicity and excellent chemical stability properties, ZnO is gaining popularity. It is crucial to properly manage the size, microstructure, and form of ZnO since these factors greatly affect its capabilities when used

as an optoelectronic material in solar cells [2][3], light-emitting diodes and photocatalysis, likewise gas sensors. Understanding the growth mechanism and morphological control of chemical bath deposition-fabricated ZnO nanostructures in detail is crucial for these applications. Chemical bath deposition (CBD) is particularly alluring because advantages over other thin film deposition processes, like its low cost, simplicity, low temperature, ease of coating of large surfaces and low evaporation temperature [4] Using hydrothermal synthesis at a low temperature (85 degrees), CBD was used to selectively produce ZnO nanorod arrays on a p-type GaN: Mg layer. Pure ZnO nanostructures exhibit weak optical properties due to point defects like interstitial Zn or oxygen vacancy, and thus cannot be used directly in the industry [5]. Doping ZnO with a useful element is thus a method for engineering optical and magnetic properties. Furthermore, n-type and p-type states are required for the fabrication of optoelectronic devices. Silver ions have two distinct properties that allow them to be used in substitution and interstitial locations, allowing them to act as acceptors in ZnO [6]. Previous research on Ag-doped ZnO researchers [7] suggested that substitutional sites were more energetically advantageous than interstitial sites. Most studies have focused on the influence of silver doping on photocatalytic activity. Effective metals and nonmetals doping of ZnO nanostructures has been widely used as an efficient method for photocatalytic activity under visible light. With this method, sunlight can be used as a low-cost, environmentally friendly energy source for photocatalytic reaction performance. The possibility of altering the electronic structure of ZnO to produce a change in the absorption edge has been investigated using both metals and nonmetals. The crystal structure, surface area, and pore [8] of ZnO can vary depending on the type of dopant used, its concentrations, and the conditions of manufacture [9][10]. The objective of the present research is to examine the optical, structural, surface morphology, and photocatalytic properties of pure and doped ZnO thin films produced via chemical bath deposition. The first sample is pure, the second

sample contains 3% Ag-doped at consistent intervals of 30 minutes, and the third sample contains 5% Ag-doped at constant intervals of 30 minutes. With the third sample now available, it is possible to compare its characteristics in this work.

MATERIALS AND METHODS

Experimental Procedure

Glass (16mm 76mm) was cleaned using deionized water, acetone, detergent solution, and ethanol wash. The glass substrates were initially submerged in a 3mol/L sodium hydroxide solution for 3 hours, then washed with deionized water (DI), subjected to an ultrasonic cleaning procedure for 15 minutes, washed once more with DI and ultrasonically, and then dried in the air. The glasses were maintained in an SnCl/HCl mixture for at least an hour prior to the experiment in order to demonstrate hydrophilic characteristics. 0.03M of a [Zn (CH₃COO) 2.2H₂O] and 0.03M of methenamine (C₆H₁₂N₄) were combined. For one hour at the necessary temperature (90 °C), In the aqueous solution, the pretreated glass substrates were placed. After the reaction, the glass substrates were taken out of the beaker and rinsed with deionized water. They were then allowed to dry in the air before being characterized or moving on to the next deposition stage. Then, different quantities of silver nitrate AgNO₃ (x = 0.03 and 0.05, respectively) were utilized to prepare the doped samples. After deposition, the substrates were raised from the bath, washed with deionized water and dried outside, then put into an airtight plastic container for storage. The morphology of the films was examined using an X-ray diffractometer and Field emission scanning electron microscopy (FESEM, JSM-5600). The Cu, K X-ray source's emission had a wavelength of 1.54° A. Photoluminescence (PL, Hitachi-S4160, Japan).

Photocatalytic activity of pure ZnO and doped silver films

The following method was used to assess the photocatalytic performance of the films as-grown: exposure to sunlight. ZnO thin films were placed in the peaker's bottom with a 50 mL

solution of methylene blue with a 30-ppm concentration, and the mixture was agitated in the dark for half an hour to promote the adsorption/desorption equilibrium process. In the month of July, between the hours of 11:00am and 12:30pm, The photodegradation experiment was carried out in direct sunlight outside. A UV-Vis spectrophotometer was used to measure the amount of MB dye in 5 mL of MB solution that was routinely at intervals of 30 minutes. The amount of MB dye was estimated based on how much of the samples' UV-Visible spectra were absorbed. Eq. 1 is used to determine the photocatalytic efficiency of as-synthesized films: Eq. (1) was used to determine the photodegradation efficiency of several Ag-doped ZnO samples:

$$\text{Degradation efficiency \%} = \frac{C_0 - C_t}{C_0} \times 100 \quad (1)$$

Here C_0 is the initial MO concentration (mg/L), and C_t shows the MO concentration (mg/L) after different intervals of UV light treatment. where η is the predicted photodegradation efficiency, C_0 is the MB dye's initial concentration, and C is the MB dye's solution concentration.

RESULT AND DISCUSSION

Structural Characteristics

XRD Patterns of pristine and Ag-doped ZnO nanoparticles is shown in Figure 1. It is clearly seen that the peaks are stronger for pure and different doping concentrations of 3% and 5% respectively, A lower Ag-doped was not used, as no change appeared on the all properties. It found that XRD peaks of ZnO (002), (110) were well matched with JCPDS 36-1451. We confirmed the hexagonal (wurtzite) crystal structure of the deposited films, in which two dominant peaks were observed at 2θ equal to the 34.421(002) plane and (110) plane [14]. Ag-doped samples expose some additional impurity peaks are presented 37.26, 45.3. The strongest peak shows that the preferential orientation is along the (111) and (102) planes. It is also seen that as the Ag-doping level increases the intensity of the peak gradually increase. The reason is that the crystallinity is increased with increasing Ag-doping concentration. The peak

(002) differs slightly by varying the doping quantity. As a result of internal stress in the lattice caused by Ag ion doping in the ZnO microparticles, the X-ray diffraction peaks in Figure.1 have shifted. The rise in Ag content from 3% to 5% also suggests a persistent rise in the intensity of silver peaks. [11].

The Average Crystal Size (D)

It is determined by the Debye-Scherrer formula by Eq. (2), and the results are shown in Table 1.

$$D = 0.94 \times \lambda / \beta \cos \theta \quad (2)$$

where, λ is the X-wavelength, θ the diffraction angle, and β is the FWHM.

The dislocation density δ was measured by Eq. (3):

$$\delta = 1/D^2 \quad (3)$$

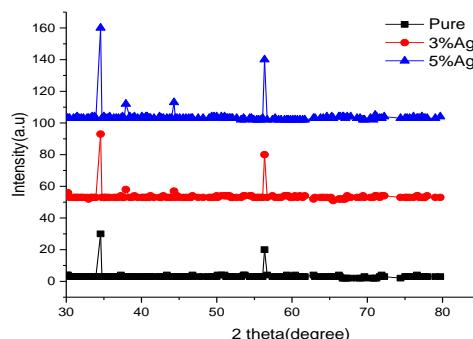


Figure 1: XRD pattern of ZnO thin films for pure, 3%, 5% Ag-ZnO thin films.

Table1: The common characteristics of pure and Ag-doped ZnO thin films, such as their typical crystalline size, FWHM, dislocation density, and strain.

No	Sample ZnO	D(nm) Avg	FWHM Avg	ϵ	δ
1	Pure	293	0.421	24	2.5
2	3% Ag	384	0.362	4.1	2
3	5% Ag	617	0.321	5.3	1.5

Optical Properties

The UV-vis optical absorption spectrum of ZnO thin films before and after being doped with silver in the wavelength range of 300-850 nm has been investigated in Figure 2. These spectra revealed that as-deposited ZnO thin films have a high absorbance of visible light, indicating their properties as an absorbing material. The energy gap change that is now available is mostly

represented by the UV-VIS absorption spectrum [12]. The wurtzite structure of ZnO may be connected to the significant UV absorption edge at 374 nm that was observed in pure ZnO thin films [13]. The absorption edge of the ZnO microparticles was shifted toward the main wavelength of 380,385nm by the addition of silver (red-shift). Doping caused variations in the absorption peaks, which revealed variations in the band structure. The altered energy gap was indicated by the shifting of the absorption edge.

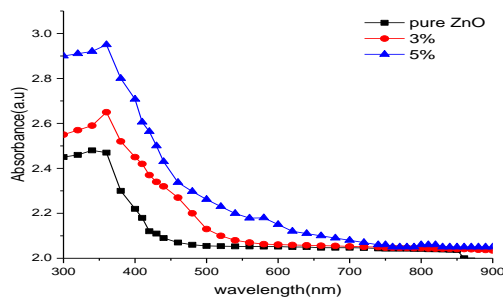


Figure 2. (a) Absorbance as a function of wavelength for pure ZnO thin films and with 3%,5% Ag-ZnO thin films.

Eq. (4) were used to estimate the absorption coefficient (α) from the absorbance (A) and thickness (t) of ZnO films. [14].

$$\alpha = 2.303 \cdot A/t \quad (4)$$

By drawing $(\alpha h\nu)^2$ versus energy, it was possible to determine the optical energy gap by Eq. (5).

$$(\alpha h\nu)^2 = B(h\nu - E_g)^{1/2} \quad (5)$$

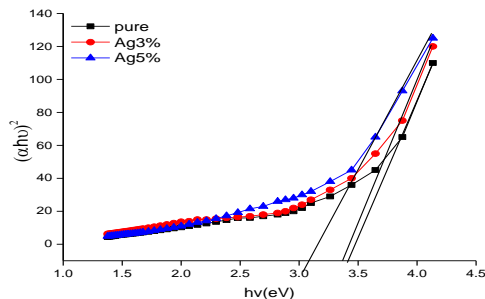


Figure 3: $(\alpha h\nu)^2$ with photon energy for silver sulphide thin films.

Figure 3 shows the difference of $(\alpha h\nu)^2$ versus energy ($h\nu$). Table 2 shows the energy gap of all samples. Figure 3 and Table 2 show that all films energy gaps decreased with doping. It should be highlighted that the efficacy of using these

materials in optoelectronic devices has grown as a result of the energy gap's reduction. [15].

Table 2: Energy band gap and crystal diameter of pure and Ag-doped ZnO microparticles.

No	Sample (ZnO)	Energy band gap (eV)	Crystal Diameter (μm)
1.	pure	3.39	11.8
2.	3%	3.34	25.61
3.	5%	3.08	31.78

Compositional analysis and Surface Morphology

The FE-SEM analysis can provide information such as shape and grain size. Figures 4(a)-(c) show FESEM images of ZnO for undoped and silver-doped ZnO microstructures. The particle sizes were clearly in the micrometer range, and the particle shapes were elliptical, quasi-spherical, or rod-shaped. It means that the particles are densely packed and randomly oriented. Figure 4 depicts the formation of elliptical and quasi-spherical microparticles with average diameters of 14-21 μm . Significant changes in the size of microparticles were observed using silver doping [16]. The non-uniform distribution of silver microparticles on the ZnO microstructure can be attributed to Ag's site selection position on ZnO. As a result, silver microparticles may form metallic clusters or tend to form microparticle agglomeration at different sites of ZnO microparticles. Agglomeration of grains may be caused by high grain sizes.



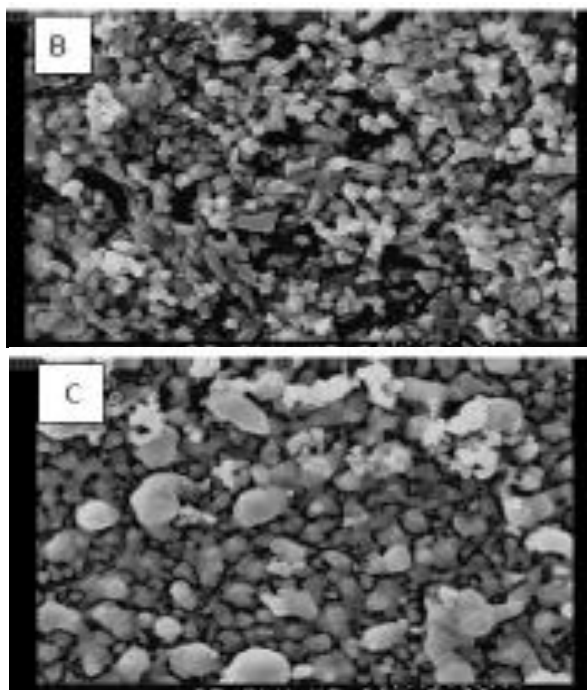


Figure 4: FESEM image of ZnO thin films (a) pure. (b) 3% Ag. (c) 5% Ag.

Photoluminescence Results (PL)

Because PL emission results from free carrier recombination, PL spectra can be used to determine the effectiveness of charge carrier immigration, transfer, and trapping as well as to comprehend what happens to electron-hole pairs in semiconductor particles. In Fig. 6, the PL spectra of pure, Ag-doped ZnO microparticles are displayed. Pure ZnO exhibits its luminous peak at 388 nm, and for Ag-doped ZnO at 410 and 430 nm, there is a notable rise in luminescence intensity because of an increase in Ag concentration, which serves as effective luminescent centers. The PL results demonstrate that rare earth elements doped with Ag are the primary luminous component and can significantly increase the luminosity of Ag-doped ZnO. There is a faint ultraviolet (UV) emission for pure ZnO microparticles at 490 nm, which is related to near band-edge emission [11]. Two strong and one weak emission at 530 nm and 410, 430 nm, respectively, were produced by the Ag-doped ZnO microparticles. Violet emission at 388nm was caused by a nihilation of excitation near the band edge of ZnO. The blue band emission at (410,430) nm was caused by surface defects in ZnO, like oxygen vacancies and zinc interstitials.

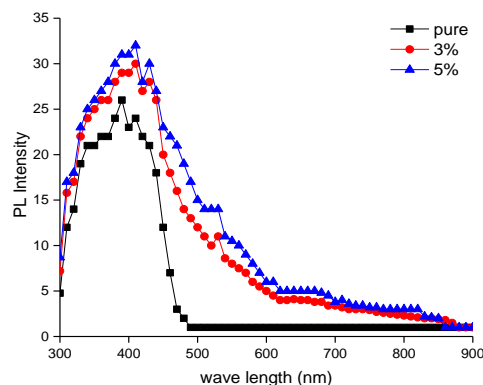


Figure 5: PL intensity for pure ZnO thin films and 3%,5% Ag-doped ZnO thin films.

Photocatalytic Activity of Ag: ZnO

The enhancement of the semiconductor materials' photocatalytic activity is attributed to a number of mechanisms. The mechanism of the photocatalytic processes is based on the electron transfer from the dye to CB of ZnO and the Fermi level of Ag, which also simultaneously makes electron transfer from CB of ZnO. Therefore, in the presence of both dye molecules and ZnO: Ag microparticles, active oxygen kinds are produced when CB electrons interact with the dissolved oxygen in the solution. The quantity of these active oxygen kinds rises with the amount of Ag, and they are in charge of the dye degradation.

Figure 5 depicts the photocatalytic activity of ZnO thin films after and before silver doping (5). After doping, the ZnO thin films have greater MB adsorption ability than before doping. These findings can be attributed to the character of each film, which is determined by its surface area [17]. In general, visible light photocatalytic reactions require a narrowing of the ZnO band gap. ZnO doping can narrow the band gap in three ways: by bringing localized energy levels into the band gap, boosting the valence band maximum, and decreasing the conduction band minimum, [8]. Although metal doping does not change the ZnO host's conduction or valence band positions, it does produce new intra-band energy levels, which are required in some applications, like the production of highly oxidized holes. The UV-VIS absorption spectra that shows the time-

based development of photodegradation of MB dye is shown in Figure 6.

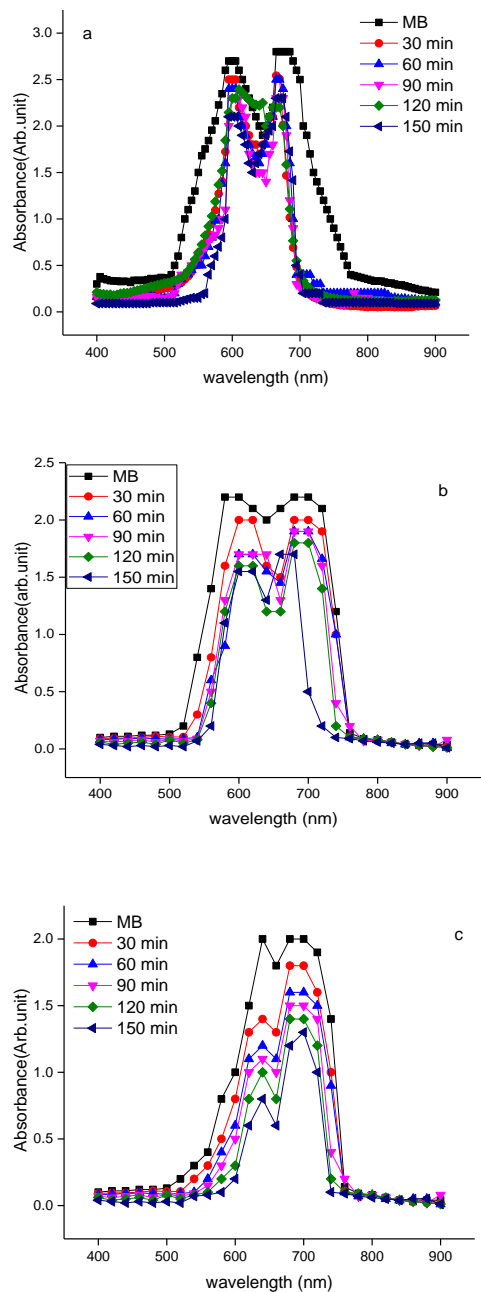


Figure 6: UV-VIS absorption spectra show the time-based development of photodegradation of MB dye. (a) pure ZnO thin films. (b) 3% Ag-ZnO thin films. (c) 5% Ag-doped ZnO thin films.

CONCLUSIONS

Investigations have been done on how Ag affects the structure and optical characteristics of ZnO. The chemical bath deposition approach was used to create pure ZnO and ZnO with varying amounts of Ag (3% and 5%). All

samples' crystallite sizes, which were calculated using Scherrer's equation, were in the micrometer range. A UV-visible spectrophotometer was used to analyze the samples' optical characteristics. Different impacts of Ag were seen on the structure, optical characteristics, and photocatalytic activities of ZnO. The typical grain sizes of pure and ZnO-doped silver range from 293 nm to 617 nm, according to investigations using scanning electron microscopy, however, they are not very consistent. Pure ZnO had a 3.3 eV energy gap. Comparing the doped samples to pure ZnO, they showed better optical characteristics. Comparing Ag-ZnO to pure ZnO, a small reduction in the energy gap was seen. Pure ZnO and Ag-doped ZnO thin films had higher photocatalytic activity, which suggests improved MB adsorption.

Disclosure and Conflicts of Interest: The authors advertise that they have no conflicts of interest.

REFERENCES

- [1] Andrzejewski, J., Pietrzyk, M. A., Jarosz, D., & Kozanecki, A, *Materials*, 2021,14(23), 7222.
- [2] service, R.F. *Science*, 1997, 276, 895.
- [3] Obreja, P., Cristea, D., Dinescu, A., & Romanitan, C., *Applied Surface Science*, 2019,463, 1117-1123
- [4] Mohammed, K. A., Al-Kabbi, A. S., & Zidan, K. M, *AIP Conference Proceedings* ,2019, Vol. 2144, 1, 030009)
- [5] Tsay, C. Y., & Yu, S. H., *Coatings*, 2021,11(10), 1259.
- [6] O. Lupan, L. Chow, L.K. Ono, B.R. Cuenya, G. Chai, H. Khallaf, S. Park, A. Schulte, Synthesis and characterization of Ag-or Sb-doped ZnO nanorods by a facile hydrothermal route, *J. Phys. Chem. C*, 2010, 114, 29, 12401–12408.
- [7] Y. Yan, M. Al-Jassim, S.-H. Wei, Doping of ZnO by group-ib elements, *Appl. Phys. Lett.* 2006,89,18, 181912.
- [8] J.M. Coronado, F. Fresno, M.D. Hernández-Alonso, R. Portela, Design of advance photocatalytic materials for energy and environmental applications, Springer, New York, 2013
- [9] C. Karunakaran, V. Rajeswari, P. Gomathisankar, Optical, electrical, photocatalytic, and bactericidal properties of microwave synthesized nanocrystalline Ag–ZnO and ZnO, *Solid State Sci.* 2011, 13, 5, 923–928.
- [10] P. Amornpitoksuk, S. Suwanboon, S. Sangkanu, A. Sukhoom, N. Muensit, *J. Powd. Technol.* 2012, 219, 158–164.

- [11] Thangaraju Chitradevi, A Jestin Lenus and N Victor Jaya, *Mater. Res. Express* 7, 2020, 015011.
- [12] HARUN GÜNEY, *Eastern Anatolian Journal of Science*, 2015, Volume I, Issue II, 77-81.
- [13] S.M. Hosseini, I. Abdolhosseini Sarsari, P. Kameli, H. Salamati, *Journal of Alloys and Compounds* 640, 2015, 408–415
- [14] B. Sathya, V. Porkalai, D. Benny Anburaj, G. Nedunchezian, *S.J. Adv. Sci. Eng.* 2017, 3 ,4 ,411-421.
- [15] Thangaraju Chitradevi, A Jestin Lenus and N Victor Jaya, *Mater. Res. Express* 7, 2020, 015011.
- [16] V. Porkalai, B. Sathya, D. Benny Anburaj, G. Nedunchezian, S. Joshua Gnanamuthu, R Meenambika, *Modern Electronic Materials*, 2018,4,4, 135–141.
- [17] Muhammad Ali Bhatti, Aqeel Ahmed Shah, Khalida Faryal Almani, Aneela Tahira, Seyed Ebrahim Chalangar, Ali Dad Chandio, Omer Nur, Magnus Willander and Zafar Hussain Ibupoto, *Ceramics International*, 2019,45,17, 23289-23297.

How to Cite

N. A. Hussain, O. A. . Dakhil, and L. Y. . Abbas, “Evaluation of the effect of Ag- doping ZnO microstructure on optical and structural properties and application in photocatalytic properties”, *Al-Mustansiriyah Journal of Science*, vol. 34, no. 3, pp. 108–114, Sep. 2023.

